A possible origin of $[M - nH + mX]^{(m-n)+}$ ions (X = alkali metal ions) in electrospray mass spectrometry of peptides

Christopher F. Rodriquez, René Fournier, Ivan K. Chu, Alan C. Hopkinson, K.W. Michael Siu*

Department of Chemistry, York University, 4700 Keele Street, Toronto, Ontario M3J 1P3, Canada

Abstract

The $[M - nH + mX]^{(m-n)+}$ (X = alkali metal ion) are common ions in the mass spectrum of a peptide that is electrosprayed in the presence of an alkali metal salt or hydroxide. The feasibility of forming $[M - nH + mX]^{(m-n)+}$ ions in the gas phase including those in the lens region of the mass spectrometer via ion–molecule reactions and/or reactions between components of collisionally activated adducts was investigated. The Li^+ ion was selected for examination since its salts are computationally the least expensive among alkali metal salts. The lithium ion affinities of the $[M - H]^-$ ions of N-methylacetamide, acetic acid, and 1-propanamine were calculated by means of density functional theory (DFT) at various levels of theory, including B3LYP/6-311++G(d, p). These three compounds were selected as representatives of relevant functional groups on a peptide. The calculated lithium ion affinities, together with evaluated thermochemical data, were used to calculate the enthalpies of reactions between the model compounds and LiOH, LiCl, and $Li(H_2O)^+$ that might lead to the formation of $[M - nH + mX]^{(m-n)+}$. A number of these reactions were found to be exothermic or slightly endothermic ($\Delta H^\circ < +20$ kcal/mol). DFT calculations on the energetics of a model reaction revealed a relatively flat potential energy hypersurface containing a well of approximately 35 kcal/mol in depth and devoid of significant barriers. These results are used to postulate the formation of $[M - nH + mX]^{(m-n)+}$ ions in the gas phase in the ion source and/or in the lens region via collisions between an ionic peptide and neutral lithium compounds or collisional activation of lithium–peptide adducts. (Int J Mass Spectrom 192 (1999) 303–317) © 1999 Elsevier Science B.V.

Keywords: Adduct ions; Alkali metal; Peptide; Collisional activation

1. Introduction

The sodium ion is an ubiquitous contaminant of samples in electrospray mass spectrometry. For peptide samples, the presence of high concentrations of Na^+ typically results in envelopes of ions of $[M - nH + mNa]^{(m-n)+}$ in the positive ion detection mode, where n is the number of protons abstracted from the peptide M, and m is the number of sodium ions incorporated [1,2]. For a given charge state, i.e. constant $(m - n)+$, the peptide containing peaks are readily identified by their separation on the m/z axis by $(23 - 1)/(m - n)$ units; however, the presence of a large number of sodium-containing adducts of the peptide crowds the mass spectrum and decreases sensitivity as the peptide signal is distributed among many peaks, and is generally considered to be a

---

* Corresponding author. E-mail: kwmsiu@yorku.ca

detriment to analytical performance [3]. For that reason, removal of Na^+ from biological samples prior to their electrospray mass spectrometric analysis is an almost universal practice [4].

Observations of metal ion-containing adducts of biomacromolecules are not restricted to those of sodium or peptides. Cations of the type, $[M - nH + mX]^{(m-n)+}$, and anions of the type, $[M - nH + mX]^{(n-m)-}$, where X = Li, K [2,5], or Ag [6], and the equivalent adduct ions where X is a divalent transition metal ion [7–11], have been reported. Furthermore, it is well known that sodium adduction is an even more common analytical problem for the analysis of oligonucleotides, which bind sodium ions via their phosphate anions in the backbone [12]. The sequestering of cations by polyanions (e.g. oligonucleotides) in solution is an interesting subject [13,14]; however, it is not known if the extent of cation binding observed in the electrospray mass spectra of oligonucleotides is entirely attributable to the polyanion effect.

There is no known *general* binding of alkali–metal ions to peptides in solution. For the *specific* cases in which *in vivo* binding is known, the numbers of bound sodium or potassium ions are small [15–17]. By contrast, it is known that transition metal ions bind strongly to peptides in solution; anchoring a transition metal ion at the N-terminus of a peptide is believed to be the first step leading to subsequent deprotonation of an amide linkage and chelation of the metal ion [18]. Similar deprotonation reactions in solution have not been reported for alkali metals despite attempts in observing them [18]. Gas-phase reactions that can lead to $[M - nH + mX]^{(m-n)+}$ are unknown. It has been argued that Coulombic repulsion between MH^+ and X^+ would preclude gas-phase reactions, and the loss of several protons in the gas phase to create anionic peptides for reaction with X^+ would be energetically prohibitive [2].

The apparent simplicity of the electrospray mass spectrum has helped to mask the complexity of electrospray mass spectrometry, which is only slowly being recognized. Smith *et al*. [3,19], Thomson [20], and Counterman *et al*. [21] have all reported dimeric protein ions that are isobaric with monomeric ions. Furthermore, Thomson [20] and Ke *et al*. [22] observed that the apparent continuous background in an electrospray mass spectrum recorded under mild lens conditions contains solvated multimetric ions of the analyte. Zhan *et al*. [23] reported re-solvation of bare electrospray-generated peptide ions in the lens region of their mass spectrometer as a result of nucleation within the supersonic expansion jet. The possibility exists that at least a portion of the solvated multimeric species observed by Thomson [20] and Ke *et al*. [22] might have been formed in the lens region via supersonic cooling.

In this article, we postulate the formation of the $[M - nH + mX]^{(m-n)+}$ ions in the gas phase in the ion source and/or in the lens region, and suggest possible reactions that may lead to their formation. Model reactions are found to be either exothermic or endothermic by less than 20 kcal/mol. Density functional theory calculations of the potential energy hypersurface of a model reaction showed that the surface contains a well of approximately 35 kcal/mol and is devoid of barriers that are larger than a few kilocalories per mole.

2. Experimental

Experiments were conducted on triple quadrupole mass spectrometers: SCIEX TAGA 6000E, PE SCIEX API365, and PE SCIEX API3000 prototype (Concord, Ontario). All oligopeptides were commercially available (Sigma, St. Louis, MO). Samples were typically 2–10 μM peptide in 50/50 water/methanol containing 10 mM of XOH or XCl (X = Li, Na, or K, Aldrich, St. Louis, MO). These were continuously infused by means of a syringe pump (Harvard Apparatus, Model 22, South Natick, MA) at a typical flow rate of 2 μL/min into an electrospray probe, with or without nebulization with air. The optimum probe position was established from time to time but was typically with the tip about 2 cm from the interface plate and with the spray off-axis from the orifice. Mass spectra were acquired in the positive ion

detection mode with unit mass resolution at a step size of 0.1 *m/z* unit and at a dwell time of 10 ms/step. Typically, ten scans were summed to produce a mass spectrum. Tandem mass spectrometry of background ions was performed on typically a 30-*m/z* window of precursor ions with a nitrogen pressure of approximately 5 mTorr in *q*2 and at a collision energy of typically 52 eV in the laboratory frame for singly charged ions.

3. Computational methods

Density functional theory employing the deMon [24–26] and GAUSSIAN 94 [27] programs was used at several different levels to calculate lithium ion affinities of $[M - H]^-$ ions derived from peptide functional groups. Test calculations with the deMon program using four different exchange-correlation functionals showed the kinetic-energy density and Laplacian dependent correlation functional of the LAP family, developed by Proynov *et al*. [28–31], when combined with the exchange functional of Becke [32] gives the best results, the calculated cation affinities being different from experimental results by 2.7 kcal/mol on average. We refer to this method by the acronym BLAP. We used a correlation consistent quintuple zeta (cc-pV5Z) basis set on atoms involved in the bonds we study and a 6-311G(d) on the other atoms. [Details about these bases and the grids and auxiliary sets used in deMon are available from one of the authors (R.F.) upon request.] In addition, we have used the hydrid B3LYP method (using Becke's three-parameter exchange functional [33] and the correlation functional from Lee *et al*. [34] and Miehlich *et al*. [35] from GAUSSIAN 94 along with 6-31++G(d, p) and 6-311++G(d, p) basis sets [36–40]. Lithium ion affinities for anions A^- are the enthalpy changes at 298 K ($\Delta H°$) for

$$Li^+A^- \rightarrow Li^+ + A^-$$

These were obtained by using the calculated electronic energies to give ΔE_{elec} values at 0 K and then

adding zero-point energies and thermal corrections [41] to convert them to $\Delta H°$ at 298 K.

4. Results and discussion

Fig. 1 shows electrospray mass spectra of (a) a cyclic decapeptide, gramicidin s, electrosprayed with 10 mM sodium hydroxide and (b) a linear nonapeptide, bradykinin, with 10 mM potassium hydroxide. In both cases, a dominant cluster of doubly charged ions and a much less abundant cluster of singly charged ions are evident. Individual peaks within the doubly charged clusters are separated by 11 and 19 *m/z* units in (a) and (b), which equal $(23 - 1)/2$ and $(39 - 1)/2$ and identify the clusters to be $[M - nH + mNa]^{(m-n)+}$ and $[M - nH + mK]^{(m-n)+}$, respectively. Reducing the alkali–metal concentrations to 1 and 0.1 mM led to lower albeit significant extents of metal incorporation; i.e. the phenomenon is not an artifact peculiar to unusually high metal-ion concentrations. Fig. 2 compares the electrospray mass spectra of bradykinin in the presence of (a) lithium hydroxide and (b) lithium chloride. In both cases the peaks are separated by $(7 - 1)/2 = 3$ *m/z* units, the fine features within a given doubly charged peak being due to a combination of ^{13}C and to a lesser extent ^6Li. It is our general observation that alkali–metal-ion containing peaks were typically more abundant when the peptide was electrosprayed with alkali–metal hydroxides rather than with alkali–metal halides.

Figs. 3 and 4 display results that reveal the complexity of electrospray mass spectrometry. The single scan mass spectrum of gramicidin s electrosprayed with potassium hydroxide in Fig. 3 was recorded with a nominally zero potential gradient in the lens region to minimize desolvation and fragmentation [22]. As previously reported [22], an elevated baseline and humps are clearly evident. Mass selecting a 30-*m/z*-unit wide window of background ions centered on *m/z* 800 for collision-induced dissociation yielded the results in Fig. 4, which shows product ion spectra (a) in the absence and (b) in the presence of 5 mTorr of
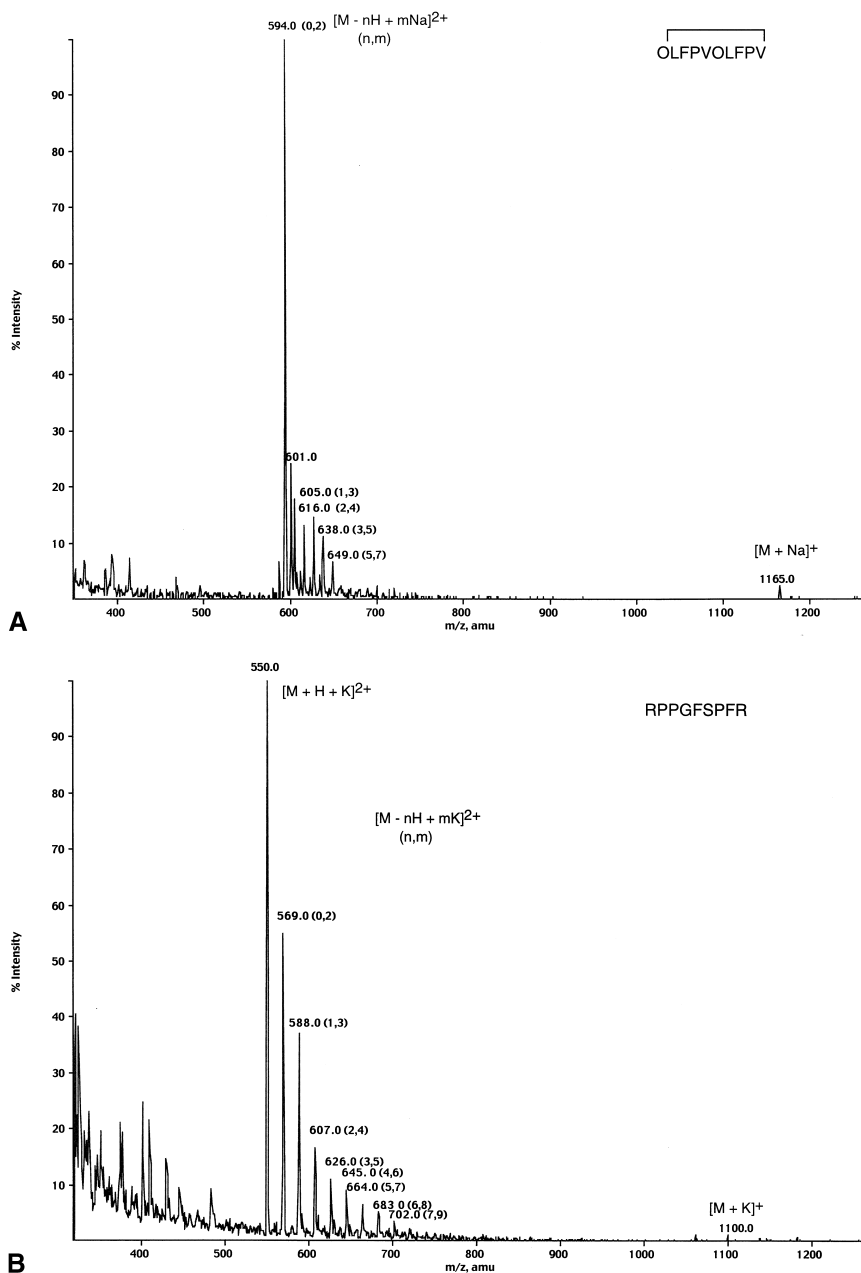
Fig. 1. Electrospray mass spectra of (a) 20 μM gramicidin s in 50/50 water/methanol adjusted to pH 12 with sodium hydroxide and (b) 20 μM bradykinin in 50/50 water/methanol adjusted to pH 12 with potassium hydroxide. The parentheses indicate (n, m) of $[M - nH + mX]^{(m-n)+}$. The peak at $m/z = 601$ in (a) is most likely due to the $[M + 2Na]^{2+}$ of a gramicidin s analogue which has a molecular mass of 14 Da higher.

nitrogen in $q2$. It is readily apparent that collision-induced dissociation of the background ions results in singly charged $[M - nH + mK]^{(m-n)+}$ ions ($m -$

$n = 1$) and $K(KOH)_p^+$ ions, where $p = 1$–4. Similar to the observation of Ke et al. [22], the location of the 30-m/z precursor ion window was not crucial; the
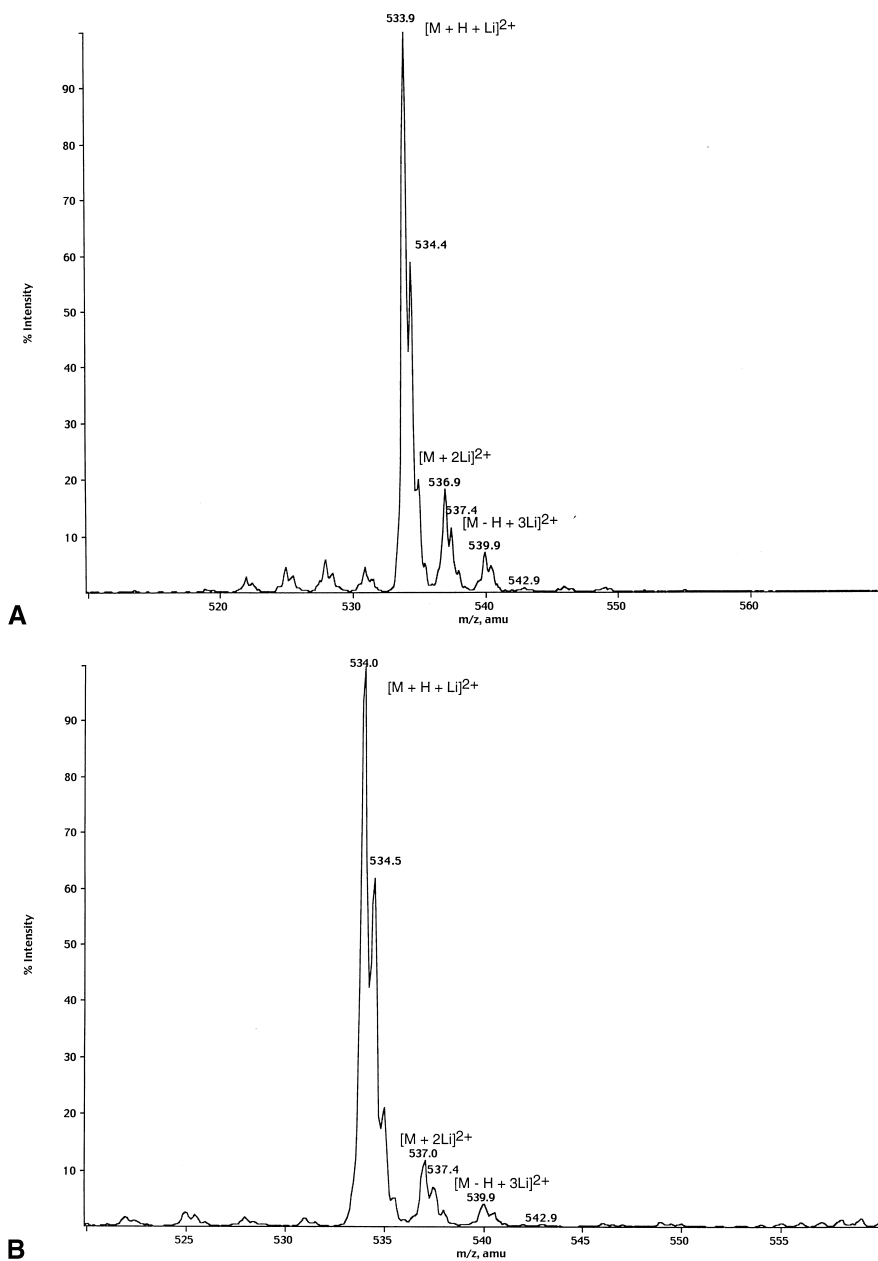
Fig. 2. Electrospray mass spectra of 10 μM bradykinin in 50/50 water/methanol with (a) 10 mM lithium hydroxide and (b) 10 mM lithium chloride.

product ion spectra of precursor window from m/z 700 to m/z 1100 were all comparable. These results support the previous speculation [20,22] that the background ions contain diverse, solvated multimers of the analyte, gramicidin s. In our example, one of the "solvents" is KOH, whose presence in the background is evident from the $K(KOH)_p^+$ ions in Fig. 4(b). As previously discussed [22], it is not known if
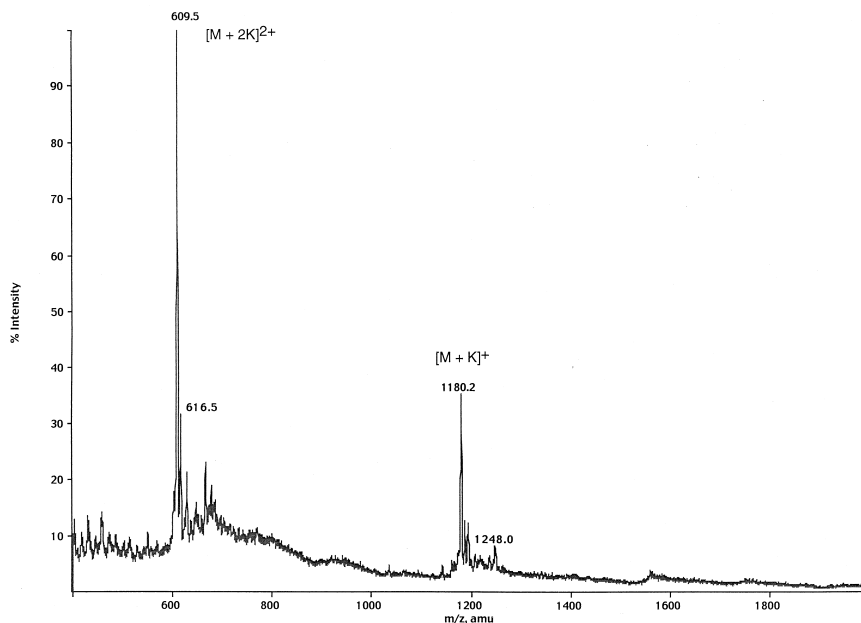
Fig. 3. Electrospray mass spectrum of 20 μM gramicidin s in 50/50 water/methanol with 10 mM potassium hydroxide acquired under nominally zero-potential-gradient conditions in the lens region of the mass spectrometer.

these solvated multimers of gramicidin s were sampled from the one atmosphere zone in the ion source or were produced in the lens region. Results of Zhan et al. [23] would indicate it was likely that at least a portion of these ionic species were formed in the lens region between bare gramicidin ion and neutral water, methanol, and/or KOH that were sampled.

The fact that adducts of the peptide, KOH, and solvent were observed, whether they be sampled or subsequently formed in the lens region, means that these components were in or could be brought in close proximity to one another within a time frame of the order of milliseconds [2]. Furthermore, ions were subjected to a large number of collisions with sampled neutral molecules both in the ion source and in the lens region before they were mass analyzed [42,43]; in case of the latter, collisional activation may overcome the barriers of endothermic reactions. Hence the possibility exists that at least a portion of the $[M - nH + mK]^{(m-n)+}$ ions could have been created in the

lens region as a result of reactions among the adduct components.

The possibility of creating $[M - nH + mX]^{(m-n)+}$ ions in the gas phase by using model molecules that mimic the functional groups on a peptide reacting with lithium hydroxide, lithium chloride, and $Li(H_2O)^+$ will be examined as follows. Lithium was chosen as the representative alkali–metal ion since it is computationally the least expensive; lithium hydroxide, lithium chloride, and $Li(H_2O)^+$ are the most likely simple species encountered in the positive ion detection mode. Hydrated species are ignored in our consideration, as we are inspecting model reactions, and their inclusion would introduce too many variables and complications.

Addition of lithium to three model $[M - H]^-$ ions, the N-methyl acetamide anion, **1**, the acetate anion, **2**, and the 1-propanamide anion, **3**, have been investigated at various levels of theory. The structural parameters obtained at different levels were all very
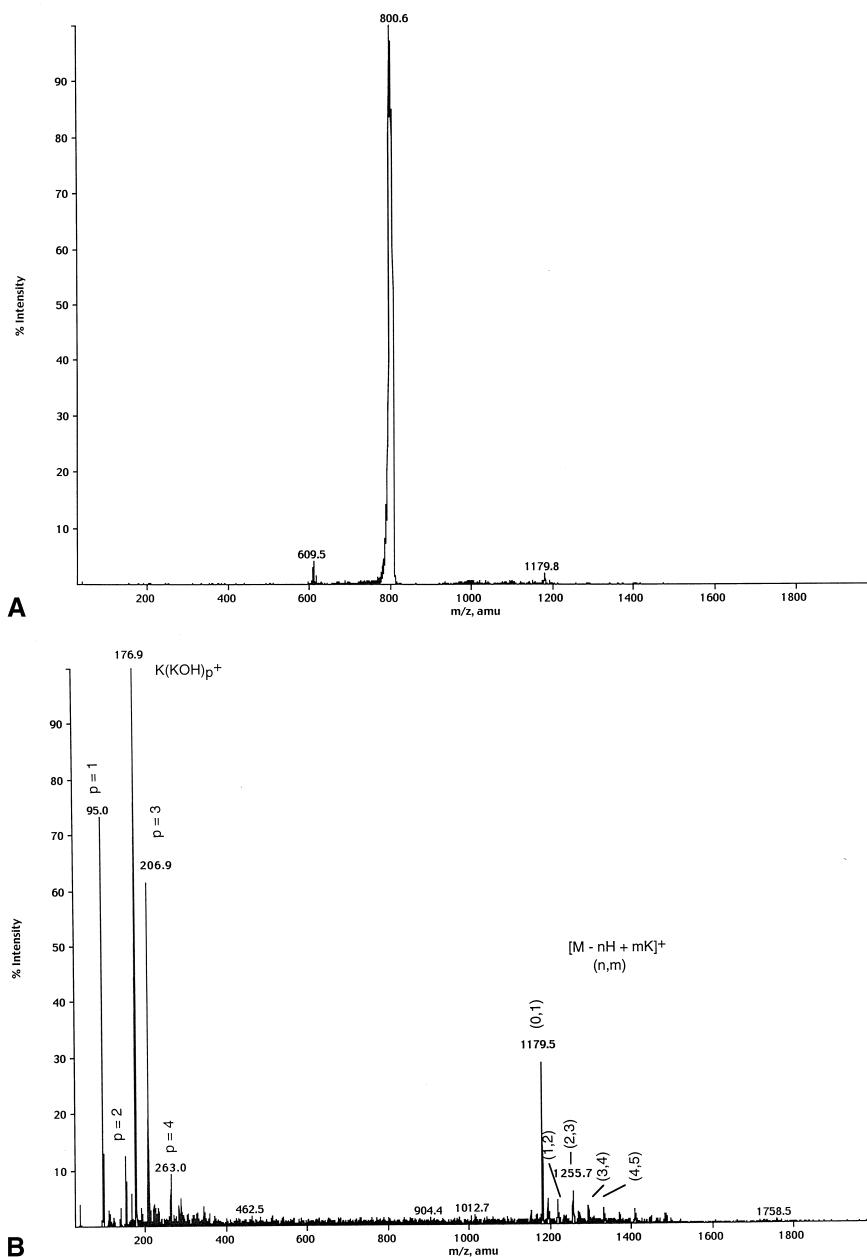
Fig. 4. Product ion spectra of a 30-*m/z*-unit wide window of background ions centering on *m/z* 800 in Fig. 3(a) in the absence of collision gas in *q*2 and (b) with 5 mTorr of nitrogen in *q*2.

similar; consequently, we report only structures (Fig. 5) and total energies (Table 1) at one level, B3LYP/ 6-311++G(*d, p*).

In anion **1** the C–O distance of 1.269 Å is consid-

erably longer than a standard carbon–oxygen double bond (1.208 Å in $H_2C=O$) [44] and the C–N distance of 1.321 Å is intermediate between standard single and double carbon–nitrogen bonds (1.471 Å in
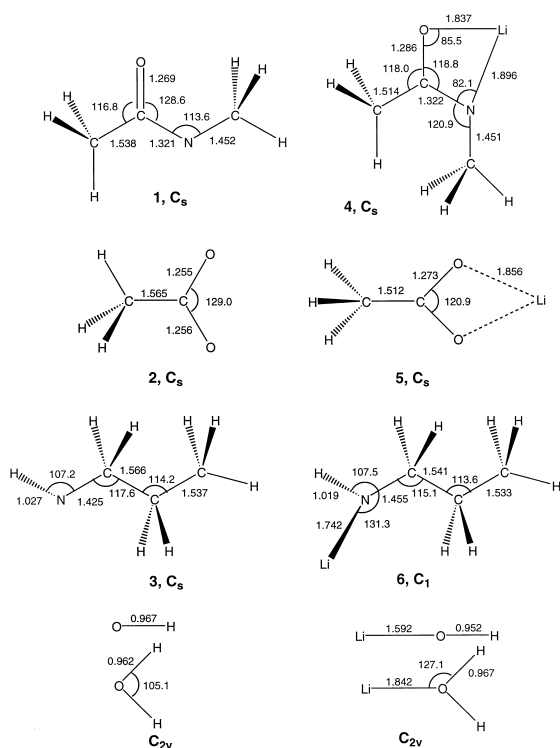
Fig. 5. Geometric parameters for anions, lithium salts, water, and $LiOH_2^+$; bond lengths are in angstroms and angles are in degrees.

H_3CNH_2 and 1.273 Å in $H_2C\!\!=\!\!NH$). These geometric parameters indicate that both resonance structures **1a** and **1b** contribute significantly to the structures of this anion.

Addition of Li^+ to anion **1** results in structure **4** where the N-methyl group bends away from the
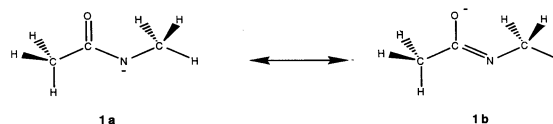
Scheme 1.

oxygen atom, i.e. unlike in the anion, the two methyl groups are *cis* to each other about the C–N double bond. This enables the lithium atom to chelate with both the oxygen and nitrogen atoms. The most notable structural change in the bond distances is for the C–O bond which is 0.017 Å longer than that in the anion. The calculated Li–O distance of 1.837 Å is considerably longer (by 0.245 Å) than that in LiOH, whereas the Li–N distance of 1.896 Å is 0.154 Å longer than that in lithium propanamide (**6**).

The carbon–oxygen distances of 1.255 and 1.256 Å in the acetate anion, **2**, are closer to a standard C–O double bond than to a single bond [44]. The almost identical bond lengths indicate approximately equal contributions from the two resonance structures **2a** and **2b**. The OCO bond angle of 129° is attributed to repulsion between the two partially negatively charged oxygen atoms.

Addition of Li^+ to **2** occurs symmetrically between the two oxygen atoms (**5**) and produces a lengthening of the C–O distances to 1.273 Å and a decrease in the OCO angle to 120.9°. Here the Li–O distances of 1.856 Å are slightly longer (by 0.019 Å) than those in the N-methylacetamide complex.

Table 1
Total energies (Hartrees) from structural optimization at B3LYP/6-311++G(*d, p*)

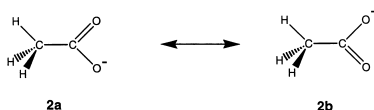| Base	Base energy	ZPE[a]	Li-Base energy[b]	Structure	ZPE[a]
1[c]	−248.016 52	54.6	−255.575 78	**4**	57.1
2[d]	−228.602 49	29.9	−236.161 68	**5**	32.3
3[e]	−173.898 47	65.0	−181.467 42	**6**	68.4
OH⁻	−75.827 45	5.4	−83.417 33		8.2
H₂O	−76.458 53	13.3	−83.801 79		15.5

[a] Zero-point energy in kcal/mol.

[b] The total energy for Li^+ is −7.284 92 Hartrees.

[c] The $[M − H]^-$ ion of N-methylacetamide.

[d] The acetate anion.

[e] The $[M − H]^-$ ion of 1-propanamine.

Scheme 2.

In the 1-propanamide anion, **3**, all four heavy atoms are coplanar. The C–N distance of 1.425 Å is 0.046 Å shorter than that in methylamine and the central C–C bond (1.566 Å) is longer than a normal single bond [44]. These bond distances are likely a result of negative hyperconjugation [45] where electron density from the lone pairs on nitrogen is donated into the σ^* orbital of the C–C bond. The net effect is an introduction of a small amount of double bond characters into the C–N bond and a weakening of the adjacent C–C bond. In the salt lithium 1-propanamide, **6**, the carbon and nitrogen atoms all remain coplanar and the N–H bond is essentially in the same location as in the anion, but with a slightly shorter bond distance. The N–Li distance of 1.742 Å is longer than that in lithium amide, $LiNH_2$. The C–N distance of 1.455 Å is closer to that of a single C–N bond [44]. Furthermore, the central C–C bond is shorter than that in the anion and is almost identical to that in ethane.

Figs. 1–4 show that a large number of alkali–metal ions may be incorporated into a nona- or decapeptide. The most common functional group on a peptide is the amide linkage on the backbone. To estimate the reaction enthalpies of the amide linkage on a peptide ion with lithium containing species, we use N-methylacetamide as our model peptide. The following three reactions will be considered:

$$CH_3CONHCH_3 + LiOH$$
$$\rightarrow CH_3CON(Li)CH_3 + H_2O \qquad (1)$$

$$CH_3CONHCH_3 + LiCl$$
$$\rightarrow CH_3CON(Li)CH_3 + HCl \qquad (2)$$

$$CH_3CONHCH_3 + Li(H_2O)^+$$
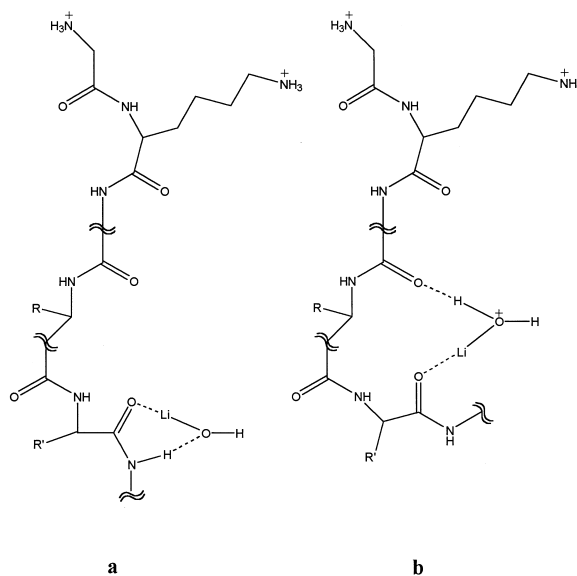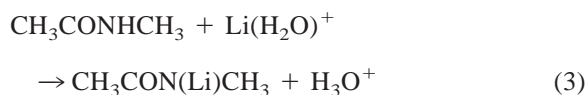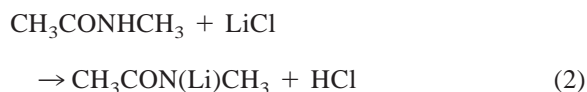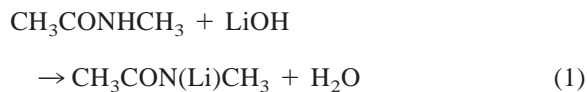$$\rightarrow CH_3CON(Li)CH_3 + H_3O^+ \qquad (3)$$

Fig. 6. Artist's rendition of (a) an adduct between a peptide ion and LiOH that is modeled by reaction (1), and (b) an adduct between a peptide ion and $Li(H_2O)^+$ that is modeled by reaction (3). Double wavy lines indicate discontinuities in the peptide structure.

Reaction (1) models the reaction between a peptide ion and lithium hydroxide that is adducted to and/or collides with it. An artist's rendition of a possible scenario where adducted LiOH on a peptide ion may react with its amide linkage is depicted in Fig. 6(a). Adduction of LiOH on the peptide ion is induced by evaporation of the solvent (thus bringing the nonvolatile LiOH molecules and the peptide ions closer to one another in solvated clusters) in the source and by condensation of LiOH on peptide ions in the lens region. Reaction (2) is a similar reaction between a peptide ion and lithium chloride. Reaction (3) models the reaction between an amide linkage on a peptide ion, whose charge centre is far removed (and hence shielded) from the linkage, and $Li(H_2O)^+$ [depicted in Fig. 6(b)] as well as that between a neutral peptide component [the two NH_3^+ groups in Fig. 6(b) are replaced by NH_2 groups] and the $Li(H_2O)^+$ component of a cluster ion.

The enthalpy changes of the reactions (1)–(3), ΔH_1°, ΔH_2°, and ΔH_3°, can be calculated from evaluated thermochemical data [46–49] plus the com-

Table 2
Evaluated reference thermochemical data employed

	Species	Value (kcal/mol)	Reference
$\Delta H^{\circ}_{\text{acid}}$			
	N-methylacetamide	361.9	[48]
	H_2O	390.7	[48]
	HCl	333.7	[48]
	CH_3COOH	348.6	[48]
	$CH_3CH_2CH_2NH_2$	398.4	[48]
LA			
	OH^-	$\Delta_f H^{\circ}(Li^+) + \Delta_f H^{\circ}(OH^-) - \Delta_f H^{\circ}(LiOH) = 162.4 - 32.7 + 56.0 = 185.7$	[46,47]
	Cl^-	$\Delta_f H^{\circ}(Li^+) + \Delta_f H^{\circ}(Cl^-) - \Delta_f H^{\circ}(LiCl) = 162.4 - 54.4 + 47.0 = 155.0$	[46–48]
	H_2O	$\Delta_f H^{\circ}(Li^+) + \Delta_f H^{\circ}(H_2O) - \Delta_f H^{\circ}(LiOH_2^+)^a = 162.4 - 57.8 - 70.7 = 33.9$	[46–49]
		$^a\Delta_f H^{\circ}(LiOH_2^+) = \Delta_f H^{\circ}(H^+) + \Delta_f H^{\circ}(LiOH) - PA(LiOH) = 365.7 - 56.0 - 239.0 = 70.7$	
PA			
	H_2O	165.0	[49]

puted lithium ion affinity of the N-methylacetamide anion:

$$\Delta H^{\circ}_1 = \Delta H^{\circ}_{\text{acid}} \text{ (amide)} + LA \text{ (OH}^-)$$
$$- \Delta H^{\circ}_{\text{acid}} \text{ (H}_2\text{O)} - LA \text{ (1)} \quad (4)$$

$$\Delta H^{\circ}_2 = \Delta H^{\circ}_{\text{acid}} \text{ (amide)} + LA \text{ (Cl}^-)$$
$$- \Delta H^{\circ}_{\text{acid}} \text{ (HCl)} - LA \text{ (1)} \quad (5)$$

$$\Delta H^{\circ}_3 = \Delta H^{\circ}_{\text{acid}} \text{ (amide)} + LA \text{ (H}_2\text{O)}$$
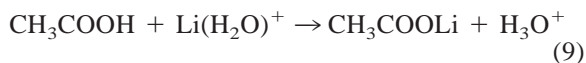$$- PA \text{ (H}_2\text{O)} - LA \text{ (1)} \quad (6)$$

where amide is N-methylacetamide, LA (1) is the lithium ion affinity of the N-methylacetamide anion, and PA is proton affinity. The appropriate values from the evaluated reference data, and the lithium ion affinities of the anions calculated using BLAP/cc-pV5Z, B3LYP/6-31++G(d, p), and B3LYP/6-311++G(d, p), are listed in Tables 2 and 3, respectively. Substituting the appropriate values in Eqs. (4), (5), and (6) and using the average lithium ion affinity of the N-methylacetamide anion yields:

$$\Delta H^{\circ}_1 = 361.9 + 185.7 - 390.7 - 169.1$$
$$= -12.2 \text{ kcal/mol}$$

$$\Delta H^{\circ}_2 = 361.9 + 155.0 - 333.7 - 169.1$$
$$= 14.1 \text{ kcal/mol}$$

$$\Delta H^{\circ}_3 = 361.9 + 33.9 - 165.0 - 169.1$$
$$= 61.7 \text{ kcal/mol}$$

To model the carboxylate functional group in the C-terminus and the side chains of aspartic and glutamic acid residues, we use acetic acid as a model. Because the carboxylate group is likely to be ionized in solution, especially in the presence of 10 mM LiOH, reactions involving both acetic acid and the acetate anion need to be considered. For neutral acetic acid, the following reactions are possible:

$$CH_3COOH + LiOH \rightarrow CH_3COOLi + H_2O \quad (7)$$

$$CH_3COOH + LiCl \rightarrow CH_3COOLi + HCl \quad (8)$$

$$CH_3COOH + Li(H_2O)^+ \rightarrow CH_3COOLi + H_3O^+ \quad (9)$$

Reactions (7) and (8) model the reactions between the carboxylic functional group of a peptide ion and, respectively, lithium hydroxide and lithium chloride that are adducted to and/or collide with the group. Reaction (9) represents the reaction between a carboxylic group that is far away from the charge centre

Table 3
Calculated LAs of anions (kcal/mol)

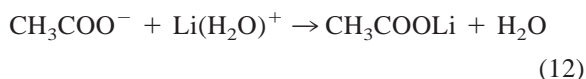| Anion	Salt	B3LYP/6-31++G(d, p)	B3LYP/6-311++G(d, p)	BLAP/cc-pV5Z	Average	Experimental[a]
1	**4**	169.6	170.4	167.3	169.1 ± 1.3[b]	
2	**5**		170.5	168.3	169.8 ± 1.1	
			170.6[c]			
3	**6**	174.0	175.6	175.1	174.9 ± 0.7	
OH$^-$	LiOH	186.1	187.9[d]	189.9	188.0 ± 1.6	185.7
H$_2$O[e]	Li(H$_2$O)$^+$	35.0	35.5	32.0	34.2 ± 1.5	33.9

[a] From Table 2.
[b] Standard deviation.
[c] MP2/6-311++G(d, p).
[d] MP4SDTQ(fc)/6-311++G($2df$, p).
[e] Neutral inserted for comparison.

of a peptide ion and Li(H$_2$O)$^+$ or that between a carboxylic group of a neutral peptide adducted to Li(H$_2$O)$^+$. The corresponding reactions for the acetate anion are

$$CH_3COO^- + LiOH \rightarrow CH_3COOLi + OH^- \quad (10)$$

$$CH_3COO^- + LiCl \rightarrow CH_3COOLi + Cl^- \quad (11)$$

$$CH_3COO^- + Li(H_2O)^+ \rightarrow CH_3COOLi + H_2O \quad (12)$$

Similarly, reactions (10) and (11) represent reactions of a carboxylate anion of an overall positively charged peptide ion with lithium hydroxide and lithium chloride adducted to and/or colliding with it whereas reaction (12) models an acetate–Li(H$_2$O)$^+$ ion pair within a lithiated cluster ion of the peptide

$$\Delta H_7^o = \Delta H_{acid}^o \text{ (acid)} + LA \text{ (OH}^-)$$
$$- \Delta H_{acid}^o \text{ (H}_2\text{O)} - LA \text{ (}\mathbf{2}\text{)}$$
$$= 348.6 + 185.7 - 390.7 - 169.8$$
$$= -26.2 \text{ kcal/mol} \quad (13)$$

$$\Delta H_8^o = \Delta H_{acid}^o \text{ (acid)} + LA \text{ (Cl}^-)$$
$$- \Delta H_{acid}^o \text{ (HCl)} - LA \text{ (}\mathbf{2}\text{)}$$
$$= 348.6 + 155.0 - 333.7 - 169.8$$
$$= 0.1 \text{ kcal/mol} \quad (14)$$

$$\Delta H_9^o = \Delta H_{acid}^o \text{ (acid)} + LA \text{ (H}_2\text{O)}$$
$$- PA \text{ (H}_2\text{O)} - LA \text{ (}\mathbf{2}\text{)}$$
$$= 348.6 + 33.9 - 165.0 - 169.8$$
$$= 47.7 \text{ kcal/mol} \quad (15)$$

$$\Delta H_{10}^o = LA \text{ (OH}^-) - LA \text{ (}\mathbf{2}\text{)}$$
$$= 185.7 - 169.8 = 15.9 \text{ kcal/mol} \quad (16)$$

$$\Delta H_{11}^o = LA \text{ (Cl}^-) - LA \text{ (}\mathbf{2}\text{)}$$
$$= 155.0 - 169.8 = -14.8 \text{ kcal/mol} \quad (17)$$

$$\Delta H_{12}^o = LA \text{ (H}_2\text{O)} - LA \text{ (}\mathbf{2}\text{)}$$
$$= 33.9 - 169.8 = -135.9 \text{ kcal/mol} \quad (18)$$

where acid is acetic acid and LA (**2**) is the lithium ion affinity of the acetate anion.

The last functional group to consider is the amino group on the side chain of lysine residues and the N-terminus. To model that functional group, we use 1-propanamine. The appropriate reactions are
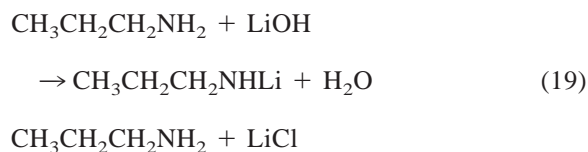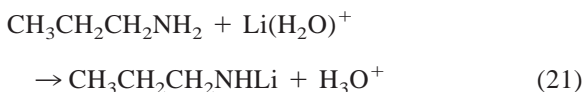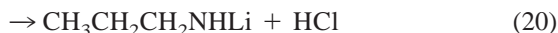
$$CH_3CH_2CH_2NH_2 + LiOH$$
$$\rightarrow CH_3CH_2CH_2NHLi + H_2O \quad (19)$$

$$CH_3CH_2CH_2NH_2 + LiCl$$

Table 4
Comparison of reaction enthalpies (kcal/mol)[a]

Species	Functional group represented	LiOH	LiCl	Li(H$_2$O)$^+$
N-methylacetamide	Peptide linkage	**−12.2**	**−14.1**	61.7
Acetic acid	Acid	**−26.2**	**0.1**	47.7
Acetate anion	Acid	**15.9**	**−14.8**	−135.9
1-propanamine	Amine	**18.5**	44.8	92.4

[a] Values that are exothermic and endothermic by less than 20 kcal/mol are shown in bold.

$$\rightarrow CH_3CH_2CH_2NHLi + HCl \tag{20}$$

$$CH_3CH_2CH_2NH_2 + Li(H_2O)^+$$

$$\rightarrow CH_3CH_2CH_2NHLi + H_3O^+ \tag{21}$$

These reactions of the amino group are equivalent to those detailed earlier for the amide linkage and the carboxylic acid group. The enthalpy changes of the reactions are

$$\Delta H_{19}^{\circ} = \Delta H_{acid}^{\circ} \, (amine) + LA \, (OH^-)$$
$$- \Delta H_{acid}^{\circ} \, (H_2O) - LA \, (\mathbf{3})$$
$$= 398.4 + 185.7 - 390.7 - 174.9$$
$$= 18.5 \text{ kcal/mol} \tag{22}$$

$$\Delta H_{20}^{\circ} = \Delta H_{acid}^{\circ} \, (amine) + LA \, (Cl^-)$$
$$- \Delta H_{acid}^{\circ} \, (HCl) - LA \, (\mathbf{3})$$
$$= 398.4 + 155.0 - 333.7 - 174.9$$
$$= 44.8 \text{ kcal/mol} \tag{23}$$

$$\Delta H_{21}^{\circ} = \Delta H_{acid}^{\circ} \, (amine) + LA \, (H_2O)$$
$$- PA \, (H_2O) - LA \, (\mathbf{3})$$
$$= 398.4 + 33.9 - 165.0 - 174.9$$
$$= 92.4 \text{ kcal/mol} \tag{24}$$

where amine is 1-propanamine and LA (**3**) is the lithium ion affinity of the 1-propanamide anion.

The enthalpy changes are tabulated in Table 4 for comparison. The enthalpies of reactions that are exothermic or endothermic by less than 20 kcal/mol are shown in bold. The centre-of-mass collision en-

ergy that a doubly charged peptide has in the lens region is typically 2–3 eV. Assuming a significant fraction of the collision energy is convertible to internal energy [50–52], it would appear reasonable that, to a first approximation, reactions that are exothermic or endothermic by less than 20 kcal/mol may be accessible in the lens region provided that the reaction barriers are not much larger than this value. The ΔS° of reactions where the number of reactants and the number of products are identical is typically small [46]. For reaction (1), ΔS° was found to be 7.1 cal/(K mol); the $T\Delta S$ term is small even when a
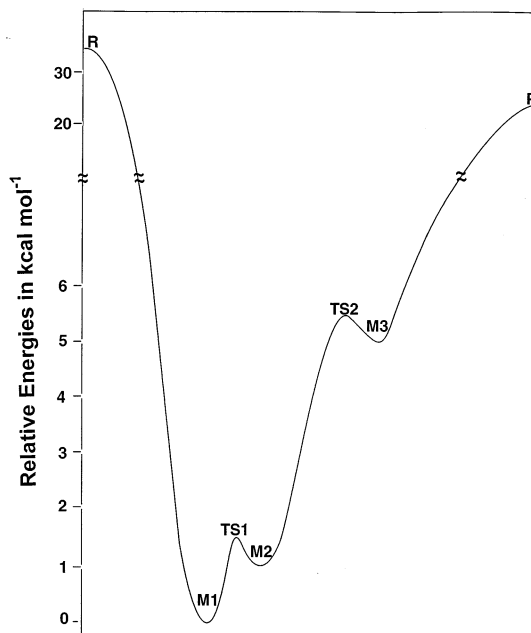

Fig. 7. Potential energy hypersurface of the reaction HCONH$_2$ + LiOH → HCON(Li)H + H$_2$O; see Fig. 8 for the structures of the minima (Ms) and the transition states (TSs).
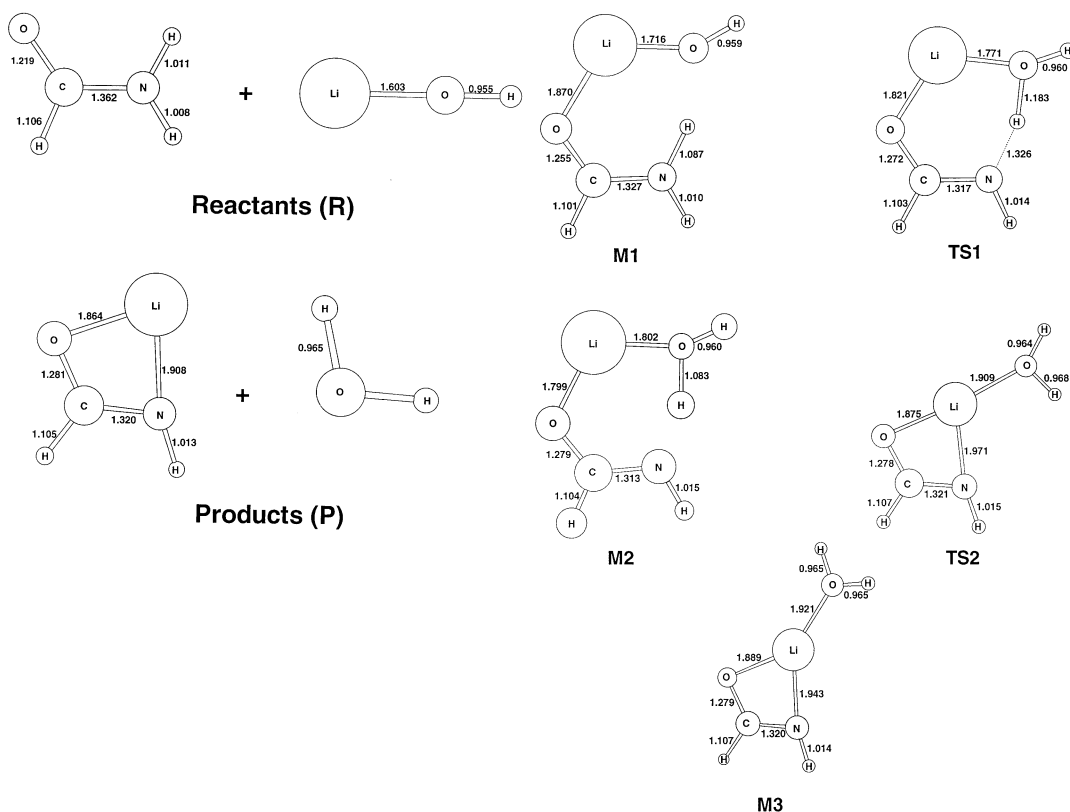
Fig. 8. Structures of reactants (R), minima (Ms), transition states (TSs) and products (P) of the lithium/hydrogen exchange reaction $HCONH_2 + LiOH \rightarrow HCON(Li)H + H_2O$; bond lengths are in angstroms.

supersonic jet temperature of much lower than 298 K is not taken into consideration. Little is known about lithium/hydrogen exchange reactions. However, it would appear reasonable to us that if the reaction barriers are not in excess of 20 kcal/mol, these reactions would probably be sufficiently efficient to occur. Calculations of the potential energy hypersurface of the model reaction:

$$HCONH_2 + LiOH \rightarrow HCON(Li)H + H_2O \qquad (25)$$

which mimics reaction (1), but is computationally more economical, reveal a surface that contains a well of about 35 kcal/mol and is devoid of significant barriers (Fig. 7, see Fig. 8 for the structures of minima and transition states and Table 5 for the energies). In fact TS1 and TS2, the transition states, disappear once zero-point vibrational energies and thermal corrections are added (results not shown). Consequently, the

reaction may be driven entirely by its exothermicity. Provided the barriers of other lithium/hydrogen exchange reactions are also small, the efficiencies of reactions (1)–(24) are determined principally by their reaction enthalpies. Furthermore, collisional activation in the lens region would allow the observation of reactions that are endothermic by less than approximately 20 kcal/mol. If this is correct, lithium hydroxide is able to react efficiently with all four species considered, lithium chloride with all but 1-propanamine, and hydrated Li^+ with only the acetate anion. By extension, lithium hydroxide will likely be able to react efficiently with all four functional groups on a peptide that these species represent, lithium chloride with all but the amino group, and hydrated Li^+ with only the carboxylate anion. The versatility of lithium hydroxide and the magnitude of its exothermicity for the peptide linkage, which is by far the most abundant

Table 5
Total electronic energies (in Hartrees), zero-point vibrational energies, and thermal corrections (both in kcal/mol) at B3LYP/6-31++G(d, p) for structures in Figs. 7 and 8

Structures	Total electronic energies[a]	Zero-point energies	Thermal corrections
R	−253.299 59 (35.4)	36.5	4.4
M1	−253.356 06 (0)	38.1	4.0
M2	−253.353 93 (1.3)	37.2	4.1
M3	−253.347 79 (5.2)	37.6	4.9
TS1	−253.353 68 (1.5)	35.7	3.8
TS2	−253.347 19 (5.6)	37.5	4.4
P	−253.319 34 (23.0)	35.9	4.4
Formamide	−169.910 92	28.5	2.4
Water	−76.434 12	13.3	1.8

[a] Relative energies in kcal/mol are in parentheses.

functional group on a peptide, is perhaps the basis for the observation that the $[M - nH + mX]^{(m-n)+}$ ions are more intense in the presence of XOH than with XCl.

Although the calculations are performed to model lithiated peptides, the conclusions are expected to be qualitatively extendable to sodium- and potassium-containing peptides. Studies into the binding of Li^+, Na^+, and K^+ to oligopeptides have shown that the alkali–metal ions all bind to ligands (at least those that are not highly basic) in a similar fashion [53–56]; it is expected that the alkali–metal ion affinities of the anions will show Li > Na > K. However, since the lithium ion affinities for the anions under consideration [LA (OH^-) = 185.7, LA (Cl^-) = 155.0, LA (N-methylacetamide anion) = 169.1, LA (acetate anion) = 169.8, and LA (1-propanamide anion) = 174.9 kcal/mol] are all comparable, it is expected that the corresponding sodium affinities and potassium affinities will exhibit similar trends. Consequently, the reaction enthalpies of the metal/hydrogen exchange reactions will probably not change drastically from lithium-, to sodium-, to potassium-containing peptides.

Acknowledgements

References

[1] G. Neubauer, R.J. Anderegg, Anal. Chem. 66 (1994) 1056–1061.
[2] J. Wang, R. Guevremont, K.W.M. Siu, Eur. Mass Spectrom. 1 (1995) 171–181.
[3] R.D. Smith, J.A. Loo, R.R. Ogorzalek Loo, M. Busman, H.R. Udseth, Mass Spectrom. Rev. 10 (1991) 359–452.
[4] T. Maniatis, E.F. Fritsch, J. Sambrook, Molecular Cloning: A Laboratory Manual, Cold Spring Harbor Laboratory, Cold Spring Harbor, NY, 1982.
[5] J. Wang, F. Ke, K.W.M. Siu, R. Guevremont, J. Mass Spectrom. 31 (1996) 159–168.
[6] H. Li, K.W.M. Siu, R. Guevremont, J.C.Y. Le Blanc, J. Am. Soc. Mass Spectrom. 8 (1997) 781–792.
[7] L.M. Teesch, J. Adams, J. Am. Chem. Soc. 112 (1990) 4110–4120.
[8] H. Zhao, J. Adams, Int. J. Mass Spectrom. Ion Processes 125 (1993) 195–205.
[9] P. Hu, M.L. Gross, J. Am. Chem. Soc. 114 (1992) 9153–9158.
[10] P. Hu, M.L. Gross, J. Am. Chem. Soc. 115 (1993) 8821–8828.
[11] O.V. Nemirovskiy, M.L. Gross, J. Am. Soc. Mass Spectrom. 9 (1998) 1285–1292.
[12] P.A. Limbach, P.F. Crain, J.A. McCloskey, J. Am. Soc. Mass Spectrom. 9 (1995) 27–39.
[13] G.S. Manning, Biopolymers 2 (1972) 937–949.

[14] G.S. Manning, Q. Rev. Biophys. II 2 (1978) 179–246.

[15] C.W. Carr, Arch. Biochem. Biophys. 62 (1956) 476–484.

[16] H. Powell Baker, H.A. Saroff, Biochemistry 4 (1965) 1670–1677.

[17] L.D. Pettit, J.E. Gregor, H. Kozlowski, in Perspectives on Bioinorganic Chemistry, R.W. Hay, J.R. Dilworth and K.B. Nolan (Eds.), Jai, London, 1991, Vol. 1, pp. 1–41.

[18] H. Sigel, R.B. Martin, Chem. Rev. 82 (1982) 385–426.

[19] R.D. Smith, K.J. Light-Wahl, B.E. Winger, J.A. Loo, Org. Mass Spectrom. 27 (1992) 811–821.

[20] B. Thomson, J. Am. Soc. Mass Spectrom. 8 (1997) 1053–1058.

[21] A.E. Counterman, S.J. Valentine, C.A. Srebalus, S.C. Henderson, C.S. Hoaglund, D.E. Clemmer, J. Am. Soc. Mass Spectrom. 9 (1998) 743–759.

[22] F. Ke, R. Guevremont, K.W.M. Siu, J. Mass Spectrom. 32 (1997) 992–1001.

[23] D. Zhan, J. Rosell, J.B. Fenn, J. Am. Soc. Mass Spectrom. 9 (1998) 1241–1247.

[24] A. St-Amant, D.R. Salahub, Chem. Phys. Lett. 169 (1990) 387–392.

[25] A. St-Amant, Ph.D. thesis, Université de Montréal, 1992.

[26] D.R. Salahub, R. Fournier, P. Mlynarski, I. Papai, A. St-Amant, J. Ushio, in Proceedings of the Ohio Supercomputer Centre Workshop on Theory and Applications of Density Functional Theory to Chemistry, J. Labanowsky and J. Andzelm (Eds.), Springer, New York, 1991.

[27] M.J. Frisch, G.W. Trucks, H.B. Schlegel, P.M.W. Gill, B.G. Johnson, M.A. Robb, J.R. Cheeseman, T. Keith, G.A. Petersson, J.A. Montgomery, K. Raghavachari, M.A. Al-Laham, V.G. Zakrzewski, J.V. Ortiz, J.B. Foresman, J. Cioslowski, B.B. Stevanov, A. Nanayakkara, M. Challacombe, C.Y. Peng, P.Y. Ayala, W. Chen, M.W. Wong, J.L. Andres, E.S. Repogle, R. Gomperts, R.L. Martin, D.J. Fox, J.S. Binkley, D.J. Defrees, J. Baker, J.P. Stewart, M. Head-Gordon, C. Gonzalez, J.A. Pople, Gaussian Inc., Pittsburgh, PA, 1995.

[28] E.I. Proynov, D.R. Salahub, Phys. Rev. B 49 (1994) 7874–7886; erratum ibid. 57 (1998) 12616.

[29] E.I. Proynov, A. Vela, D.R. Salahub, Chem. Phys. Lett. 230 (1994) 419–428; erratum, ibid. 234 (1995) 462–462.

[30] E.I. Proynov, E. Ruiz, A. Vela, D.R. Salahub, Int. J. Quant. Chem. (Symp.) 29 (1995) 61.

[31] E.I. Proynov, S. Sirois, D.R. Salahub, Int. J. Quant. Chem. 64 (1997) 427–446.

[32] A.D. Becke, Phys. Rev. A 38 (1988) 3098–3100.

[33] A.D. Becke, J. Chem. Phys. 98 (1993) 5648–5652.

[34] C. Lee, W. Yang, R.G. Parr, Phys. Rev. B 37 (1988) 785–789.

[35] B. Miehlich, A. Savin, H. Stoll, H. Preuss, Chem. Phys. Lett. 157 (1989) 200–206.

[36] R. Krishnan, J.S. Binkley, R. Seeger, J. Pople, J. Chem. Phys. 72 (1980) 650–654.

[37] A.D. McLean, G.S. Chandler, J. Chem. Phys. 72 (1980) 5639–5648.

[38] J. Chandrasekhar, J.G. Andrade, P.v.R. Schleyer, J. Am. Chem. Soc. 103 (1981) 5609–5612.

[39] J. Chandrasekhar, G.W. Spitznagel, P.v.R. Schleyer, J. Comput. Chem. 4 (1983) 294–301.

[40] L.A. Curtiss, M.P. McGrath, J.P. Blaudeau, N.E. Davis, R.C. Binning Jr., L. Radom, J. Chem. Phys. 103 (1995) 6104–6113.

[41] D.A. McQuarrie, Statistical Mechanics, Harper & Row, New York, 1976, p. 156.

[42] D.J. Douglas, J.B. French, J. Am. Soc. Mass Spectrom. 3 (1992) 398–408.

[43] T. Covey, D.J. Douglas, J. Am. Soc. Mass Spectrom. 4 (1993) 616–623.

[44] All "standard" bond lengths were taken from compilations in W.J. Hehre, L. Radom, P.v.R. Schleyer, J.A. Pople, Ab Initio Molecular Orbital Theory, Wiley-Interscience, New York, 1986.

[45] P.v.R. Schleyer, A.J. Kos, Tetrahedron 39 (1983) 1141–1150.

[46] S.G. Lias, J.E. Bartmess, J.F. Liebman, J.L. Holmes, R.D. Levin, W.G. Mallard, J. Phys. Chem. Ref. Data 17, Suppl. 1, 1988.

[47] S.G. Lias, J.F. Liebman, R.D. Levin, S.A. Kafafi, NIST Standard Reference Database 25, Version 2.02, 1994.

[48] J.E. Bartmess, NIST Standard Reference Database 19B, Version 3.01, 1993.

[49] E.P. Hunter, S.G. Lias, NIST Chemistry WebBook, http://webbook.nist.gov/chemistry; E.P. Hunter and S.G. Lias, J. Phys. Chem. Ref. Data 27 (1998) 413–656.

[50] E.M. Marzluff, S. Campbell, M.T. Rodgers, J.L. Beauchamp, J. Am. Chem. Soc. 116 (1994) 6947–6948.

[51] Y.-L. Chen, J.M. Campbell, B.A. Collings, L. Konermann, D.J. Douglas, Rapid Commun. Mass Spectrom. 12 (1998) 1003–1010.

[52] R.M.A. Heeren, K. Vékey, Rapid Commun. Mass Spectrom. 12 (1998) 1175–1181.

[53] F. Jensen, J. Am. Chem. Soc. 114 (1992) 9533–9537.

[54] S. Bouchonnet, Y. Hoppilliard, Org. Mass Spectrom. 27 (1992) 71–76.

[55] G. Bojesen, T. Breindahl, U.N. Andersen, Org. Mass Spectrom. 28 (1993) 1448–1452.

[56] P. Kebarle, J. Mass Spectrom. 32 (1997) 922–929.